Chemical Science

ROYAL SOCIETY OF CHEMISTRY

EDGE ARTICLE

View Article Online
View Journal | View Issue

Cite this: *Chem. Sci.*, 2024, **15**, 20573

All publication charges for this article have been paid for by the Royal Society of Chemistry

Received 4th June 2024
Accepted 15th November 2024

DOI: 10.1039/d4sc03665d

rsc.li/chemical-science

Aluminium porphyrins catalyse the hydrogenation of CO_2 with H_2†

Nitin Kumar, [a] Gabriela Gastelu, [b] Martin Zábranský, [a] Jaroslav Kukla, [c] Jorge G. Uranga *[b] and Martin Hulla *[a]

Boron-based frustrated Lewis pairs (FLPs) have become well-established catalysts for the hydrogenation of a wide range of functional groups. Conversely, aluminium-based FLP hydrogenation catalysts are less common, especially for CO_2 reduction. They are mostly confined to the hydrogenation of imines, alkenes, and alkynes even though aluminium is much more abundant than boron and forms structurally related compounds. Moreover, aluminium forms penta- and hexa-coordinated complexes, which remain untested in FLP hydrogenation catalysis. Herein, we demonstrate that cationic, hexa-coordinated diaqua-*meso*-tetraphenylporphyrin aluminium complexes [Al(TPP)$(OH_2)_2$]X and [Al(^{t}BuTPP)$(OH_2)_2$]X (X = Cl^-, OTf^-, ClO_4^-) form FLPs with nitrogen bases, activate H_2, and reductively couple CO_2 to amines, yielding *N*-formylamines and water. Our experimental results and DFT analysis indicate that H_2 activation involves the formation of an FLP, base-promoted CO_2 reduction and formate salt elimination from the FLP, as proposed for transition metal-catalyzed *N*-formylations. These similarities in the reaction mechanism and structure of aluminium complexes brings Al-based FLPs closer to transition metal catalysis and may enable us to apply this knowledge to ligand design to enhance main group metal-promoted hydrogenations.

Introduction

Frustrated Lewis pairs (FLPs) are combinations of Lewis acids (LA) and bases (LB) sterically hindered from generating classical LA-LB adducts. FLPs have been used to activate small molecules,[1] especially H_2,[2,3] and to catalyse hydrogenations.[4] As a case in point, boron-based FLPs catalytically hydrogenate ketones, esters, imines, enamines, *N*-heterocyclic compounds, silyl ethers, oxime ethers, alkenes, alkynes, aromatics and to some extent even CO_2.[5–8] In contrast, functional aluminium-based FLP hydrogenation catalysts remain rare, even though aluminium is chemically related to and, by far, much more abundant than boron.

In fact, aluminium is the most abundant metal in the Earth's crust and, like boron, forms predominantly trivalent compounds, which are LAs and, as such, potentially suitable for FLP chemistry. Aluminium-based FLPs are well established[9,10] and known to facilitate hydroborations,[11–13] to react with ammonia boranes,[14] C–H,[15,16] C≡C,[17,18] C=O[19–21] bonds and CO_2 (ref. 22–25) and even to activate H_2,[12,26] in some cases.

Produced in the same reaction, Al-hydrides are, however, less stable than B-hydrides (*c.f.* $NaBH_4$ and $LiAlH_4$),[27] and Al–C bonds of parent LAs are less thermally and hydrolytically stable than their boron equivalents.[28,29] For example, $B(C_6F_5)_3$ can be used as the LA component of FLP hydrogenation catalysts at temperatures up to 100 °C, even in wet solvents,[30,31] while $Al(C_6F_5)_3$ decomposes at 60 °C, facilitating only the stoichiometric reduction of alkenes.[32]

Alkenes have been catalytically reduced by incorporating three coordinate aluminium catechol LAs into porous organic polymers (Scheme 1a), but this approach failed to hydrogenate other substrates, such as ketones and imines.[33] By then, though, imine hydrogenation had already been catalysed by Al-based FLPs, with di-isobutylaluminium hydride and tri-isobutylaluminium (DIBAL, TIBAL) LAs at 103 bar of H_2.[34] More recently, this system has also proved effective with $MAlH_4$ (M = Li, Mg, Ca, Sr) at 1 bar of H_2 (Scheme 1b).[35,36] Under these reaction conditions, aluminium likely binds to the imine substrate, thereby forming an FLP suitable for H_2 activation.[37,38] Imine hydrogenation has also been catalysed by [(^{Dipp}BIAN)Al-$(H)_2$–Li$(OEt_2)_2$][39] at 50 bar of H_2 and 100 °C and by cationic (β-diketiminate)$AlMe^+$ (ref. 40) at 1.5 bar of H_2 and 60 °C, but attempts at expanding the scope of hydrogenation activity beyond imines, alkenes and alkynes have not been successful

[a]*Department of Inorganic Chemistry, Faculty of Science, Charles University, Albertov 6, 128 00 Praha 2, Czech Republic. E-mail: martin.hulla@natur.cuni.cz*

[b]*Instituto de Investigaciones en Físico-Química Córdoba Universidad Nacional de Córdoba (INFIQC-CONICET), Córdoba, 5000, Argentina. E-mail: jorge.uranga@unc.edu.ar*

[c]*Institute for Environmental Studies, Faculty of Science, Charles University, Albertov 6, 128 00 Praha 2, Czech Republic*

† Electronic supplementary information (ESI) available. CCDC 2357273, 2357274 and 2386191. For ESI and crystallographic data in CIF or other electronic format see DOI: https://doi.org/10.1039/d4sc03665d

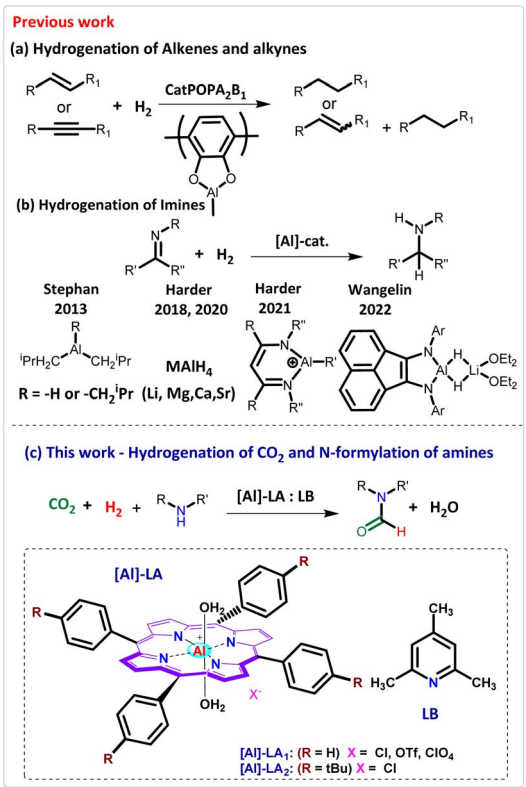

Scheme 1 (a) Hydrogenation of alkenes and alkynes; (b) hydrogenation of imines by Al-based catalysts; (c) *N*-formylation of amines with CO_2 and H_2 catalysed by Al-porphyrin.

thus far.[40] In other words, Al-catalysed hydrogenations continue to fail when applied to other substrates, such as aldehydes, ketones and CO_2, and succeed only with catechol-borane when using Al-based FLPs.[29,41,42]

In this study, we demonstrate that cationic, hexa-coordinate diaqua Al-porphyrin complexes form FLPs with nitrogen bases, activate H_2, and act as CO_2 hydrogenation catalysts in the presence of amines, yielding *N*-formylamines and water (Scheme 1c). Our experimental results and DFT analysis indicate that weaker bases, such as 2,4,6-collidine (p*K*a of conjugate acid 7.43 in H_2O), activate H_2 more readily than morpholine (p*K*a of conjugate acid 8.36 in H_2O) or 1,8-diazabicyclo[5.4.0] undec-7-ene (DBU p*K*a of conjugate acid 23.9 in MeCN), which bind to CO_2 and the LAs and hinder H_2 activation. Furthermore, the *N*-formylation reaction proceeds as proposed for well-established transition metal catalysts,[43–59] suggesting that the hexa-coordinate aluminium complexes behave as transition metals in hydrogenation chemistry. Combined, our findings may stimulate ligand and catalyst design knowledge transfer from the field of transition metal catalysis to FLPs.

Result and discussion

Diaqua-*meso*-tetraphenylporphyrin aluminium complexes [Al(TPP)$(OH_2)_2$]X, where X = Cl^-, OTf^-, ClO_4^- and diaqua-*meso*-tetra(4-*tert*-butylphenyl)porphyrin aluminium chloride

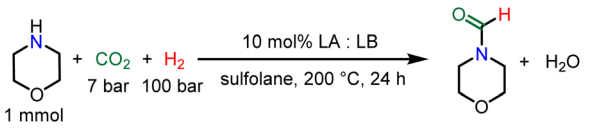

Scheme 2 Standard reaction conditions for the study of Al-based FLPs in the *N*-formylation reaction of morpholine.

[Al(^{t}BuTPP)$(OH_2)_2$]Cl, were prepared as reported in the literature (ESI†).[60] *N*-formylation of morpholine with CO_2 and H_2 was selected as the initial model hydrogenation reaction because CO_2 reduction is particularly challenging with FLPs[5,7,61] but well established with main group hydrides.[62] For the reaction to proceed, these main group hydrides must be formed during FLP-catalysed hydrogenation from H_2. The preliminary reaction conditions (1 mmol of morpholine, 10 mol% of [[Al(TPP)$(OH_2)_2$]Cl:2,4,6-collidine], 4 bar of CO_2, 96 bar of H_2, 180 °C, 4 mL of sulfolane) were selected based on the only FLP hydrogenation catalyst [R_3SnX:2,4,6-collidine] known for this reaction.[63] Under these conditions, the desired product, *N*-formylmorpholine, was synthesized in 33% yield, a value that is below average as the yields reported for [R_3SnX:2,4,6-collidine] FLPs range from 39 to 95%, depending on the R and X groups.[63]

Moreover, [[Al(TPP)$(OH_2)_2$]Cl:2,4,6-collidine] and [[Al(TPP)$(OH_2)_2$]Cl:morpholine] can be formed in the system (*vide infra*) and act as FLP in H_2 activation and CO_2 reduction, as confirmed by the results. At RT, the Lewis bases deprotonate the aqua ligands, but at high temperatures, the same ligands are reversibly displaced (ESI†). Minor adjustments were then made to the reaction conditions to suit the Al-porphyrin system (Scheme 2) before introducing structural modifications to the LA and LB used as the FLP catalyst (Table 1).

Under these modified conditions and with [Al(TPP)$(OH_2)_2$]Cl, *N*-formylmorpholine was formed in 60% yield (Table 1, entry 1). Substituting the counter anion Cl^- for OTf^- or ClO_4^- decreased the yield to 44 and 24%, respectively (Table 1, entries 2 and 3). By contrast, the ions OTf^- and ClO_4^- interact less in the tetra-substituted R_3SnX (X = Cl^-, OTf^-, ClO_4^-), accelerating the catalytic turnovers.[63] During catalysis, the counter anion likely interacts with the cationic complex [Al(TPP)$(OH_2)_2]^+$ and promotes the reaction, as shown by adding tetrabutylammonium chloride (10 mol%) to [Al(TPP)$(OH_2)_2$]OTf, which increases the reaction yield from 44 to 50% (ESI†).

In addition, the axial ligand of the porphyrin complex must be labile because the stable [Al(TPP)(OH)] complex is inactive (Table 1, entry 12). Together with morpholinium or collidinium chloride, [Al(TPP)(OH)] may be a reaction intermediate (*vide infra*). But adding morpholinium chloride to the *N*-formylation reaction with [Al(TPP)(OH)] and 2,4,6-collidine does not promote formamide formation (Table 1, entry 13). Therefore, [Al(TPP)(OH)] should not be formed during the reaction.

Substituting the *meso*-tetraphenylporphyrin ligand for *meso*-tetra(4-*tert*-butylphenyl)porphyrin [Al(^{t}BuTPP)$(OH_2)_2$]Cl slightly decreased the catalytic activity, leading to 53% *N*-formyl morpholine yield (Table 1, entry 4). The electron-donating *tert*-butyl group on the porphyrin ligand likely diminishes the Lewis

Table 1 The structures of LA and LB affect the *N*-formylation of morpholine with CO_2 and H_2[a]

Entry	LA	Added LB	Yield (%)	Error[b] (σ)
1	[Al(TPP)$(OH_2)_2$]Cl	2,4,6-col.	60	4
2	[Al(TPP)$(OH_2)_2$]OTf	2,4,6-col.	44	2
3	[Al(TPP)$(OH_2)_2$]ClO_4	2,4,6-col.	24	2
4	[Al(^{t}BuTPP)$(OH_2)_2$]Cl	2,4,6-col.	53	1
5	[Al(Pht)Cl]	2,4,6-col.	19	1
6	[Al(TPP)$(OH_2)_2$]Cl	—	26	2
7	[Al(TPP)$(OH_2)_2$]Cl	DBU	30	5
8	[Al(TPP)$(OH_2)_2$]Cl	NMM	15	4
9	[Al(TPP)$(OH_2)_2$]Cl	2,6-Lut	20	6
10	TPP	2,4,6-col.	4	—
11	—	2,4,6-col.	4	—
12	[Al(TPP)(OH)]	2,4,6-col.	4	—
13	[Al(TPP)(OH)] + [morpholineH]Cl	2,4,6-col.	4	—

[a] Reaction conditions: morpholine (1 mmol), sulfolane (4 mL), LA and LB (10 mol%), CO_2 (7 bar), H_2 (100 bar), 200 °C, 24 h, average yield after three runs. [b] The error indicated is one standard deviation rounded to a whole number. Yield was determined by ^{1}H NMR with an internal standard.

acidity of the complex, decreasing the activity. The commercial phthalocyanine complex [Al(Pht)Cl] further decreased the yield of *N*-formylmorpholine to only 19% (Table 1, entry 5).

Considering that porphyrins and phthalocyanines are planar, steric hindrance should not account for the decrease in reactivity. This difference more likely derives from electronic effects associated with changes in the LA of the metal centre and, above all, from the cationic charge of $[Al(TPP)(OH_2)_2]^+$, which enthalpically promotes the reaction (*vide infra*).

FLP catalysts can also be electronically controlled by LB, so we assessed the LB effect on the reaction. Two possible FLPs can be formed in the *N*-formylation of morpholine with [Al(TPP)$(OH_2)_2$]X and 2,4,6-collidine, namely [[Al(TPP)(OH_2)] Cl:2,4,6-collidine] and [[Al(TPP)(OH_2)]Cl:morpholine], since the reaction substrate is also a LB. Moreover, morpholine is a stronger base (p*K*a 8.36) than 2,4,6-collidine (p*K*a 7.43) and, accordingly, should more efficiently activate H_2 in combination with LA. Yet, when 2,4,6-collidine was removed from the reaction mixture, the product yield decreased from 60 to 26% (Table 1, entries 1 and 6), indicating that 2,4,6-collidine is crucial for the reaction.

Morpholine may react with CO_2, forming a carbamic acid, which removes the base from the reaction, thereby preventing FLP formation.[63] This hypothesis was partly supported by the lack of changes in yield when using stronger bases, such as DBU (p*K*a 23.9 in MeCN). DBU also reacts with CO_2, forming carbamates and the desired product in 30% yield, which was as high as that obtained when running the reaction without DBU (Table 1, entry 7). In turn, *N*-methylmorpholine (NMM, p*K*a 7.38) and 2,6-lutidine (p*K*a 6.6) decreased the yield to 15 and 20%, respectively (Table 1, entries 8 and 9). Although aliphatic NMM and 2,4,6-collidine have similar basicities (p*K*a of conjugate acid in H_2O of 7.38 and 7.43, respectively), NMM is presumably not sterically hindered enough for FLP formation. By contrast, 2,6-lutidine has the same steric profile as 2,4,6-collidine but is too weak of a LB.

When optimizing the reaction conditions, we observed that the reaction only proceeded at temperatures above 160 °C, suggesting a high energy barrier (Fig. 1A). In line with the ease of CO_2 reduction by main group hydrides,[62,63] the reaction readily proceeded at low CO_2 partial pressures between 2 and 10 bar (Fig. 1B). Conversely, transition metal-catalysed reactions usually require a high CO_2 partial pressure, typically between 25

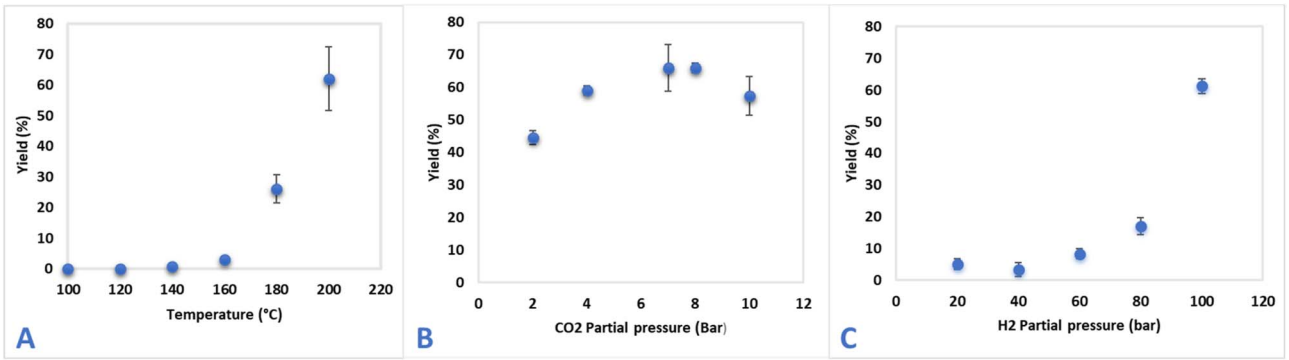

Fig. 1 Effect of H_2 (C) and CO_2 (B) partial pressure and temperature (A) on the *N*-formylation reaction of morpholine with CO_2, H_2 and [Al(TPP)$(OH_2)_2$]Cl catalyst. All yields were determined by ^{1}H NMR with an internal standard as the averages of three runs, and with error bars representing one standard deviation.

and 30 bar.[43–59] Nevertheless, high partial pressures of H_2 are required to improve the *N*-formylmorpholine yield from 4% at 20 bar to 60% at 100 bar (Fig. 1C), further indicating that H_2 activation or its binding is, most likely, limiting the reaction.

Despite extensive efforts to optimize the conditions, the reaction yields did not surpass 60% (Fig. 1). Neither prolonging the reaction nor adding more catalyst, whether [Al(TPP)$(OH_2)_2$]Cl or 2,4,6-collidine, increased the yield. Thus, reaction equilibria, not insufficient reaction time or catalyst instability, accounted for the maximum reaction yield.

Knowing that the reaction is thermodynamically favourable, we studied its mechanism in detail using both experimental approaches and DFT calculations (Fig. 2). Numerous reaction pathways have been hypothesized for *N*-formylations catalysed by FLPs, which differ in CO_2 reduction and *N*-formylation steps.[63] The first, main group-like hydride reduction of CO_2, presumably involves CO_2 insertion into the Al–H bond and [Al(TPP)(OCHO)] and [baseH]Cl formation followed by a reaction with morpholine, yielding the desired *N*-formylmorpholine, [Al(TPP)(OH)] and [baseH]Cl. The catalyst is regenerated by water elimination from [Al(TPP)(OH)] through protonation with [baseH]Cl. Nevertheless, [Al(TPP)(OH)] is catalytically inactive in the presence of an equimolar quantity of [baseH]Cl (Table 1, entry 13). Even with a 10-fold excess morpholinium chloride, required for [Al(TPP)(OH)] protonation, the reaction is slower than with [Al(TPP)$(OH_2)_2$]Cl, so [Al(TPP)(OH)] formation is unlikely to significantly contribute to the reaction. Similarly, the second reaction pathway *via* direct carbamate reduction leads to inactive [Al(TPP)(OH)]. Both reaction pathways contradict the experimental results and are, therefore, unlikely to be the working catalytic cycles.

The third catalytic cycle includes H_2 splitting, subsequent CO_2 reduction to formate, formate release and regeneration of the initial FLP, which closes the catalytic cycle. To gain further insights into the third reaction mechanism, we performed solvation-corrected DFT calculations at the M06-2X/6-311++G** level of theory so as to describe the enthalpy of the reaction coordinate at 473 K and 100 bar (ESI†). At first, the effect of 2,4,6-collidine on the reaction was studied using [Al(TPP)Cl:morpholine] *i.e.*, without 2,4,6-collidine (Fig. 2, blue pathway), and with [Al(TPP)Cl:2,4,6-collidine] FLP when this base was present (Fig. 2, orange pathway). The effect of the cationic complex [Al(TPP)$(OH_2)_2$]Cl, replacing the neutral [Al(TPP)Cl], was then assessed on the more favourable pathway in the presence of 2,4,6-collidine (Fig. 2, green pathway).

In the presence of a LB, morpholine (B_a) or 2,4,6-collidine (B_b), [Al(TPP)Cl] immediately completes its coordination sphere, forming a hexa-coordinate octahedral complex (Fig. 3, $\mathbf{R_a}$ and $\mathbf{R_b}$), as observed in transition metal catalysts during the *N*-formylation reaction.[64] In the presence of morpholine, this complex is stabilized by −24.8 kcal mol^{-1} (Fig. 2, $\mathbf{R_a}$), with a bond length between morpholine and the aluminium centre of 2.17 Å and an almost straight angle of 177.3° between TPP and the aluminium centre (Fig. 3, $\mathbf{R_a}$). Similar energetics are found for morpholinium carbamate binding (−25.4 kcal mol^{-1}), suggesting reversible CO_2 insertion into the Al-morpholine bond (ESI†). In contrast, the

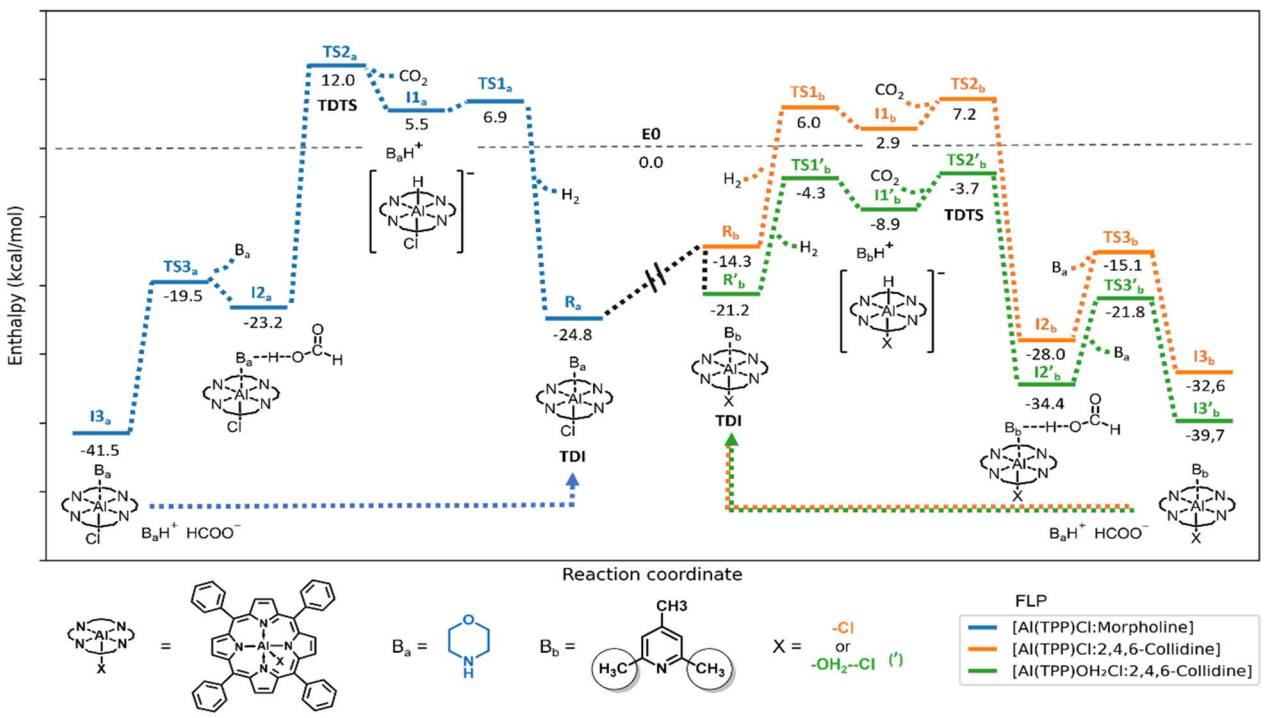

Fig. 2 DFT study of the reaction mechanism of *N*-formylation of morpholine with CO_2 and H_2 catalyzed by Al-based FLPs at the M06-2X/6-311++G** level of theory, using IEFPCM model for solvation corrections; the reaction pathway with [Al(TPP)Cl:morpholine] FLP is indicated in blue (left-hand side), the one with [Al(TPP)Cl:2,4,6-collidine] FLP is indicated in orange and the one with [[Al(TPP)(OH_2)]Cl:2,4,6-collidine] FLP is indicated in green (right-hand side). Relative enthalpies are indicated in kcal mol^{-1}, and E0 represents the sum of the enthalpies of the initial compounds without any interaction between them.

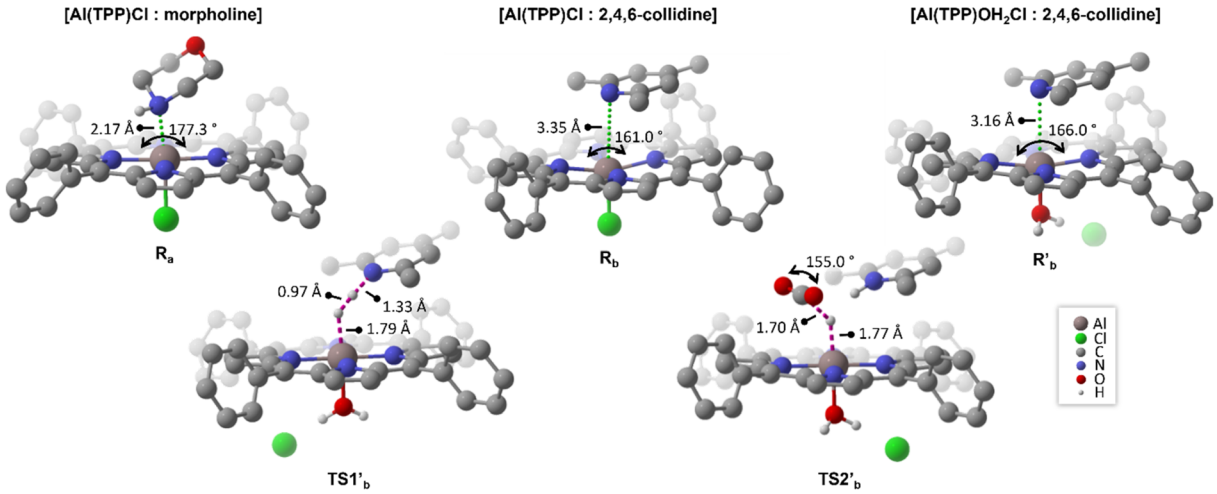

Fig. 3 Optimized geometries of [Al(TPP)Cl:morpholine] ($\mathbf{R_a}$), [Al(TPP)Cl:2,4,6-collidine] ($\mathbf{R_b}$) and [[Al(TPP)(OH_2)]Cl:2,4,6-collidine] (**R'b**) (top), and the corresponding transition states for H_2 splitting and CO_2 hydrogenation for [[Al(TPP)(OH_2)]Cl:2,4,6-collidine] catalysts ($TS1'_b$ and $TS2'_b$) (bottom). C–H hydrogens are omitted for a better visualization, at the M06-2X/6-311++G** level of theory, using IEFPCM model for solvation corrections.

octahedral complex with 2,4,6-collidine is stabilized by only −14.3 kcal mol^{-1} (Fig. 2, $\mathbf{R_b}$). Since $\mathbf{R_b}$ can be converted into $\mathbf{R_a}$, $\mathbf{R_a}$ acts as an off-cycle intermediate for the catalytic cycle with 2,4,6-collidine. In $\mathbf{R_b}$, the distance between 2,4,6-collidine and aluminium is 3.35 Å, and the distortion from octahedral geometry is larger, with an angle of 161.0° between TPP and aluminium (Fig. 3, $\mathbf{R_b}$). As previously proposed,[65,66] the distance between 3 and 5 Å is optimal for H_2 activation by FLP and, accordingly, favoured by $\mathbf{R_b}$.

H_2 activation proceeds in a heterolytic fashion.[66,67] H_2 activation from $\mathbf{R_a}$ has a higher energy transition state (Fig. 2, $\mathbf{TS1_a}$) than H_2 activation from $\mathbf{R_b}$ (Fig. 2, $\mathbf{TS1_b}$). The local activation barrier for direct H_2 activation from $\mathbf{R_a}$ is 31.7 kcal mol^{-1}, and only 20.3 kcal mol^{-1} from $\mathbf{R_b}$. Moreover, considering the equilibrium between $\mathbf{R_a}$ and $\mathbf{R_b}$, the energy barrier for H_2 activation from $\mathbf{R_a}$ is favoured by its transformation to $\mathbf{R_b}$, followed by H_2 activation *via* $\mathbf{TS1_b}$, with the energy barrier (30.8 kcal mol^{-1}) mildly favouring this process. The Al-hydrides, $\mathbf{I1_a}$ and $\mathbf{I1_b}$, are formed in endothermic reactions with relative enthalpies of 5.5 and 2.9 kcal mol^{-1}, respectively. Based on these positive energies, their formation is enthalpically unfavourable, so they are likely rapidly protonated by $[baseH]^+$ or by the ever present carbamic acid, which is produced in the reaction of morpholine with CO_2.

Al-hydride protonation is a standard decomposition pathway of such compounds.[27] Hydrides of comparably planar calix[4]pyrrole aluminium complexes exist only in an unfavourable equilibrium and are rapidly displaced by even weakly basic ligands, such as THF.[27,68] An unfavourable pre-equilibrium between H_2 and Al-hydrides, $\mathbf{I1_a}$ and $\mathbf{I1_b}$, is thus expected, where $\mathbf{I1_b}$ is slightly favoured over $\mathbf{I1_a}$ and should persist longer or in larger quantities in the reaction. Together with the high local activation energy for H_2 activation, the unfavourable pre-equilibrium is likely responsible for the high H_2 partial pressure(s) required for the reaction. Experimentally, dihydrogen activation is confirmed when using D_2, which results in complete deuteration of the formamide moiety of *N*-formylmorpholine. Thus, dihydrogen is the sole source of reducing agent of the reaction (ESI†).

The high reactivity of Al-hydrides produced in the reaction is also clearly shown by the low local activation barrier for CO_2 reduction (Fig. 2, $\mathbf{TS2_a}$ and $\mathbf{TS2_b}$). Although most Al-hydrides formed in this reaction are likely protonated back to H_2 in the reverse reaction, this reaction can proceed thanks to the comparably low local energy barriers of CO_2 reduction (6.5 and 4.3 kcal mol^{-1}, respectively). Attempts at isolating [Al(H)(TPP)] failed, but adding CO_2 to the solution led to its immediate reduction to formate, as detected by ^1H NMR (ESI†).

Based on the enthalpic energetic span of the catalytic cycle, the transition states $\mathbf{TS2_a}$ and $\mathbf{TS2_b}$ for CO_2 reduction are also the turnover frequency (TOF)-determining transition states (TDTS), with a global energy barrier of 36.8 kcal mol^{-1} starting from the TOF-determining intermediate (TDI) $\mathbf{R_a}$ *via* $\mathbf{TS1_a}$ and $\mathbf{I1_a}$. For the 2,4,6-collidine pathway (orange), the global energy barrier is only 21.5 kcal mol^{-1} between $\mathbf{R_b}$ and $\mathbf{TS2_b}$ *via* $\mathbf{TS1_b}$ and $\mathbf{I1_b}$. Alternatively, the energy span from $\mathbf{R_a}$ to $\mathbf{TS2_b}$ *via* $\mathbf{R_b}$, $\mathbf{TS1_b}$ and $\mathbf{I1_b}$ is 32.0 kcal mol^{-1} considering the equilibrium between $\mathbf{R_b}$ and $\mathbf{R_a}$ and the ability of $\mathbf{R_a}$ to act as an off-cycle thermodynamic well for the 2,4,6-collidine pathway. In effect, the reaction with 2,4,6-collidine is favoured in all cases, in line with the experimental results (Table 1, entries 1 and 6).

After $\mathbf{TS2_a}$ and $\mathbf{TS2_b}$, stable, intermediate complexes between [Al(TPP)Cl], formic acid and morpholine ($\mathbf{I2_a}$) or 2,4,6-collidine ($\mathbf{I2_b}$) are formed. With morpholine, $\mathbf{I2_a}$ has a stabilization energy similar to that of $\mathbf{R_a}$ (−23.2 *vs.* −24.8 kcal mol^{-1}, respectively), potentially allowing the reverse reaction. The reverse reaction, HCOOH decomposition to CO_2 and H_2, is also well established in the literature[69] and was confirmed here by evolution of H_2 gas, characterized by ^1H NMR, from a solution of formic acid and $[Al(TPP)(OH_2)_2]Cl$ (ESI†). Considering these

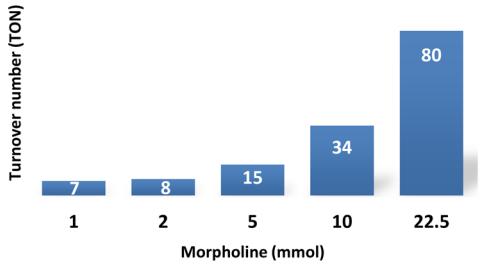

Fig. 4 Morpholine effect on the TON of the catalytic system; TON calculated based on the quantity of $[Al(TPP)(OH_2)_2]Cl$ under the following reaction conditions: morpholine (1 to 22.5 mmol), sulfolane (4 mL), [[Al(TPP)(OH_2)]Cl:2,4,6-collidine] (0.1 mmol), CO_2 (7 bar), H_2 (100 bar), 200 °C, 24 h. The reaction yield was determined by ^{1}H NMR with an internal standard.

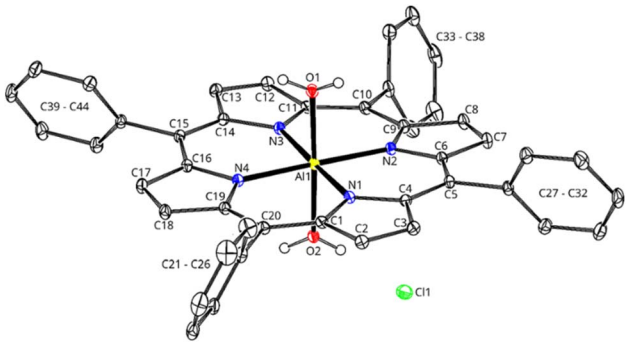

Fig. 5 View of the molecular structure of $[Al(TPP)(OH_2)_2]Cl$ as observed in the crystal structure of $[Al(TPP)(OH_2)_2]Cl \cdot CH_2Cl_2 \cdot 2\ Et_2O$. C–H hydrogen atoms were omitted for clarity. Thermal displacement ellipsoids are plotted at the 30% probability level. Applied colours: C – black, H – black contour, Cl – green, N – blue, O – red, Al – yellow.

results, a thermodynamic equilibrium may be established in the reaction, thereby limiting the reaction yield.

Thermodynamically, the reaction is driven by [morpholinium][formate] elimination from either $\mathbf{I2_a}$ or $\mathbf{I2_b}$, which spontaneously condenses into *N*-formylmorpholine and water under these reaction conditions.[47,64] This condensation also regenerates the FLP catalyst and allows the reaction to proceed. Formate salts are eliminated in transition metal-catalysed reactions,[47,64] whereas the formate remains attached to the central element[70–72] in reactions of main group hydrides, including $LiAlH_4$,[73] so the [Al(TPP)Cl] catalyst behaves like a transition metal rather than a main group reductant. In the-complex **I2**, the protonated base continuously interacts with the LA and the generated formate. Therefore, another base, such as morpholine, is required for the reaction to proceed (Fig. 2, $\mathbf{TS3_{a\ and\ b}}$) prior to catalyst regeneration.

If the reaction is limited by an equilibrium established between $\mathbf{R_{(a\ or\ b)}}$ and $\mathbf{I2_{(a\ or\ b)}}$ and driven by morpholine, higher concentrations of morpholine should promote the reaction. Indeed, increasing the quantity of morpholine increased the turnover number (TON) in the 24 hours reaction (Fig. 4). More specifically, increasing the substrate concentration from 1 to 22.5 mmol increased the TON from 7 to 80. This increase confirmed that the 60% yield obtained with 1 mmol of morpholine (Table 1, entry 1) is limited by the quantity of the substrate, not by the efficiency of the catalyst.

In the catalytic cycle with the $[Al(TPP)(OH_2)_2]Cl$ pre-catalyst (Fig. 5), dissociation of one aqua ligand leads to the [[Al(TPP)(OH_2)]Cl:2,4,6-collidine] FLP ($\mathbf{R'_b}$), whose geometry is similar to, but more stable than, that of [Al(TPP)Cl:2,4,6-collidine] ($\mathbf{R_b}$) (Fig. 3). Nevertheless, the subsequent transition states, $\mathbf{TS1'_b}$ and $\mathbf{TS2'b}$ (Fig. 3), are more stabilized (Fig. 2, $\mathbf{TS1'b}$ and $\mathbf{TS2'b}$), lowering the overall activation barrier of the catalytic cycle. The H_2 splitting step proceeds *via* a late transition state $\mathbf{TS1'b}$, wherein the H–H bond is 0.2 Å more stretched than in H_2. Despite having the largest local activation barrier (16.9 kcal mol^{-1}), this transition *via* $\mathbf{TS1'b}$ is still much more energetically favourable than the transition from the neutral complex $\mathbf{R_b}$ to $\mathbf{TS1_b}$ (20.3 kcal mol^{-1}). In comparison with the neutral $\mathbf{TS2_b}$, $\mathbf{TS2'b}$ stabilization decreases the energetic span of the catalytic cycle from 21.5 ($\mathbf{R_b} \rightarrow \mathbf{TS2_b}$) to 17.5 ($\mathbf{R'b} \rightarrow \mathbf{TS2'b}$) kcal mol^{-1}. When including potential off-cycle intermediates, $\mathbf{R_a}$ and $\mathbf{R'a}$, where morpholine binds to the catalyst, the energy span decreases from 32.0 ($\mathbf{R_a} \rightarrow \mathbf{R_b} \rightarrow \mathbf{TS2_b}$) to 29.4 ($\mathbf{R'a} \rightarrow \mathbf{R'b} \rightarrow \mathbf{TS2'b}$) kcal mol^{-1} (ESI†). This difference supports our hypothesis that the cationic aqua complexes of aluminium and the associated FLP with collidine [[Al(TPP)(OH_2)]Cl:2,4,6-collidine] is the most favourable catalyst in the system.

While the DFT calculations fit the experimental data, the pathways involve, at most, tri-molecular transition states and the formation of an Al-hydride. $[Al(TPP)(OH_2)]Cl$ is a hard LA, whose interactions with the relatively soft hydride donor are potentially less favourable than with the considerably harder CO_2. Alternative pathway(s) may involve H_2 activation by a tetra-molecular transition state involving CO_2 interactions with the Al-catalyst and H_2 activation by the C-atom of CO_2 and the LB, resulting in the direct CO_2 reduction to formate. Such a possibility is currently under investigation in our laboratory.

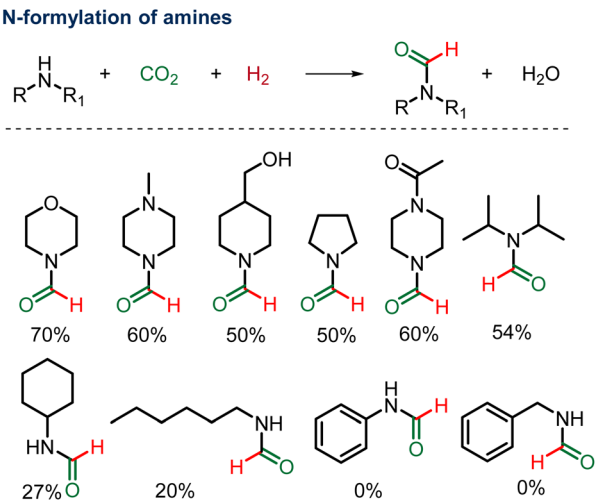

Scheme 3 Substrate scope (a) *N*-formylation of amines with CO_2 and H_2. Reaction conditions: amine (1 mmol), sulfolane (4 mL), [[Al(TPP)(OH_2)]Cl:2,4,6-collidine] (10 mol%), CO_2 (7 bars), H_2 (100 bars), 200 °C, 24 h. All yields were determined by ^{1}H NMR, and the structures were confirmed by GC-MS.

After studying the catalytic system, we assessed the substrate effect on the *N*-formylation of amines with CO_2 and H_2 (Scheme 3). In the *N*-formylation reaction, all secondary amines tested yielded the corresponding *N*-formylated products between 40 and 60% yield, in line with the expected reaction equilibrium. The alcohol, tertiary amine and amide functional groups were well tolerated. Diisopropyl amine was almost unreactive in the only other FLP system reported thus far, namely [R_3SnX:2,4,6-collidine].[63] But in our system, due to its low steric hindrance around the LA centre, diisopropyl amine provided an average yield of 54%. Primary aliphatic amines were also *N*-formylated for the first time with FLP catalysts, albeit in yields ≤20%. Aromatic and benzylic amines were unreactive.

Conclusion

Hexa-coordinated complexes of aluminium incorporating a labile ligand such as water can be used as LAs in FLP chemistry, H_2 activation, and hydrogenation chemistry. Catalytic hydrogenation of CO_2 in the presence of amines yields formamides with [Al(TTP)$(OH_2)_2$]Cl as the Lewis acid and the sterically demanding 2,4,6-collidine as the Lewis base. Energetically, the reaction is favoured when using the cationic complex [Al(TTP)$(OH_2)_2$]Cl over the neutral [Al(TPP)Cl], which is also unstable and hydrolyses to the cationic form. The advantages of this FLP system are the absence of labile and hydrolytically unstable Al–C bonds, which allows hydrogenation reactions that produce water. Structural and reactivity similarities of the LAs to transition metal complexes may facilitate knowledge transfer from transition metal catalysis to FLP in ligand and catalyst design. Ligand modifications may enable us to tailor Lewis acidity and steric hindrance around the metal centre to improve the reactivity of FLPs and to tune their reactivity to reaction requirements.

Data availability

All the data supporting this article have been included in the main text and the ESI.†

Author contributions

The manuscript was written through contributions of all authors. All authors have given approval to the final version of the manuscript.

Conflicts of interest

There are no conflicts to declare.

Acknowledgements

We thank the Czech Science foundation (GAČR 21-27431M) for funding this study, the National Scientific and Technical Research Council (Consejo Nacional de Investigaciones Científicas y Técnicas – CONICET) for Gabriela Gastelu's fellowship and Charles University Research Centre program No. UNCE/24/SCI/010 for supporting Martin Zábranský. We also thank Carlos V. Melo for editing the manuscript and Alexandros Paparakis for preparing 4-piperidinemethanol, which was used in the substrate scope. This research relied on computational resources of the High-Performance Computing Center (Centro de Computación de Alto Desempeño – CCAD) of the National University of Córdoba (Universidad Nacional de Cordoba – UNC) (**https://ccad.unc.edu.ar/**), part of the National System of High-Performance Computing (Sistema Nacional de Computación de Alto Desempeño – SNCAD) of the Ministry of Science, Technology and Innovation (Ministerio de Ciencia, Tecnología e Innovación – MinCyT), Argentina.

References

1 D. W. Stephan and G. Erker, *Chem. Sci.*, 2014, **5**, 2625–2641.
2 D. W. Stephan and G. Erker, *Angew. Chem., Int. Ed.*, 2010, **49**, 46–76.
3 D. W. Stephan, *J. Am. Chem. Soc.*, 2021, **143**, 20002–20014.
4 J. Lam, K. M. Szkop, E. Mosaferi and D. W. Stephan, *Chem. Soc. Rev.*, 2019, **48**, 3592–3612.
5 A. E. Ashley, A. L. Thompson and D. O'Hare, *Angew. Chem., Int. Ed.*, 2009, **48**, 9839–9843.
6 M. A. Courtemanche, A. P. Pulis, É. Rochette, M. A. Légaré, D. W. Stephan and F. G. Fontaine, *Chem. Commun.*, 2015, **51**, 9797–9800.
7 T. Wang, M. Xu, A. R. Jupp, Z. W. Qu, S. Grimme and D. W. Stephan, *Angew. Chem., Int. Ed.*, 2021, **60**, 25771–25775.
8 J. Lam, K. M. Szkop, E. Mosaferi and D. W. Stephan, *Chem. Soc. Rev.*, 2019, **48**, 3592–3612.
9 M. J. Ingleson, *Annu. Rep. Prog. Chem., Sect. A. Inorg. and Phys. Chem.*, 2013, **109**, 28–52.
10 S. A. Weicker and D. W. Stephan, *Bull. Chem. Soc. Jpn.*, 2015, **88**, 1003–1016.
11 D. M. C. Ould, J. L. Carden, R. Page and R. L. Melen, *Inorg. Chem.*, 2020, **59**, 14891–14898.
12 G. Ménard, L. Tran and D. W. Stephan, *Dalton Trans.*, 2013, **42**, 13685–13691.
13 N. Sarkar, R. Kumar Sahoo and S. Nembenna, *Chem.–Eur. J.*, 2023, **29**, e202203023.
14 C. Appelt, J. C. Slootweg, K. Lammertsma and W. Uhl, *Angew. Chem., Int. Ed.*, 2013, **52**, 4256–4259.
15 G. Ménard, J. A. Hatnean, H. J. Cowley, A. J. Lough, J. M. Rawson and D. W. Stephan, *J. Am. Chem. Soc.*, 2013, **135**, 6446–6449.
16 G. Ménard and D. W. Stephan, *Angew. Chem., Int. Ed.*, 2012, **51**, 4409–4412.
17 Y. Chen, W. Jiang, B. Li, G. Fu, S. Chen and H. Zhu, *Dalton Trans.*, 2019, **48**, 9152–9160.
18 C. Appelt, H. Westenberg, F. Bertini, A. W. Ehlers, J. C. Slootweg, K. Lammertsma and W. Uhl, *Angew. Chem., Int. Ed.*, 2011, **50**, 3925–3928.
19 M. Lange, J. C. Tendyck, P. Wegener, A. Hepp, E.-U. Würthwein and W. Uhl, *Chem.–Eur. J.*, 2018, **24**, 12856–12868.

20 D. Pleschka, M. Layh, F. Rogel and W. Uhl, *Philos. Trans. R. Soc., A*, 2017, **375**, 20170011.
21 W. Uhl, P. Wegener, M. Layh, A. Hepp and E. U. Würthwein, *Z. Naturforsch., B: Chem. Sci.*, 2016, **71**, 1043–1050.
22 G. Ménard, T. M. Gilbert, J. A. Hatnean, A. Kraft, I. Krossing and D. W. Stephan, *Organometallics*, 2013, **32**, 4416–4422.
23 P. Federmann, T. Bosse, S. Wolff, B. Cula, C. Herwig and C. Limberg, *Chem. Commun.*, 2022, **58**, 13451–13454.
24 P. Federmann, R. Müller, F. Beckmann, C. Lau, B. Cula, M. Kaupp and C. Limberg, *Chem.–Eur. J.*, 2022, **28**, e202200404.
25 S. Roters, C. Appelt, H. Westenberg, A. Hepp, J. C. Slootweg, K. Lammertsma and W. Uhl, *Dalton Trans.*, 2012, **41**, 9033–9045.
26 S. Styra, M. Radius, E. Moos, A. Bihlmeier and F. Breher, *Chem.–Eur. J.*, 2016, **22**, 9508–9512.
27 M. M. D. Roy, A. A. Omaña, A. S. S. Wilson, M. S. Hill, S. Aldrich and E. Rivard, *Chem. Soc. Rev.*, 2021, **121**, 12784–12965.
28 N. A. Shcherbina, A. V. Pomogaeva, A. S. Lisovenko, I. V. Kazakov, N. Yu. Gugin, O. V. Khoroshilova, Y. V. Kondrat'ev and A. Y. Timoshkin, *Z. Anorg. Allg. Chem.*, 2020, **646**, 873–881.
29 M. A. Courtemanche, J. Larouche, M. A. Légaré, W. Bi, L. Maron and F. G. Fontaine, *Organometallics*, 2013, **32**, 6804–6811.
30 D. J. Scott, T. R. Simmons, E. J. Lawrence, G. G. Wildgoose, M. J. Fuchter and A. E. Ashley, *ACS Catal.*, 2015, **5**, 5540–5544.
31 T. Mahdi and D. W. Stephan, *J. Am. Chem. Soc.*, 2014, **136**, 15809–15812.
32 G. Ménard and D. W. Stephan, *Angew. Chem.*, 2012, **124**, 8397–8400.
33 J. Camacho-Bunquin, M. Ferrandon, U. Das, F. Dogan, C. Liu, C. Larsen, A. E. Platero-Prats, L. A. Curtiss, A. S. Hock, J. T. Miller, S. T. Nguyen, C. L. Marshall, M. Delferro and P. C. Stair, *ACS Catal.*, 2017, **7**, 689–694.
34 J. A. Hatnean, J. W. Thomson, P. A. Chase and D. W. Stephan, *Chem. Commun.*, 2014, **50**, 301–303.
35 H. Elsen, C. Färber, G. Ballmann and S. Harder, *Angew. Chem., Int. Ed.*, 2018, **57**, 7156–7160.
36 H. Elsen, J. Langer, M. Wiesinger and S. Harder, *Organometallics*, 2020, **39**, 4238–4246.
37 H. Elsen, J. Langer, G. Ballmann, M. Wiesinger and S. Harder, *Chem.–Eur. J.*, 2021, **27**, 401–411.
38 Z. Qu, H. Zhu and S. Grimme, *ChemCatChem*, 2021, **13**, 3401–3404.
39 J. Pölker, D. Schaarschmidt, J. Bernauer, M. Villa and A. Jacobi von Wangelin, *ChemCatChem*, 2022, **14**, e202200144.
40 A. Friedrich, J. Eyselein, H. Elsen, J. Langer, J. Pahl, M. Wiesinger and S. Harder, *Chem.–Eur. J.*, 2021, **27**, 7756–7763.
41 F. Krämer, *Angew. Chem., Int. Ed.*, 2024, **63**, e202405207.
42 F. Krämer, J. Paradies, I. Fernández and F. Breher, *Chem.–Eur. J.*, 2024, **30**, e202303380.
43 P. Ju, J. Chen, A. Chen, L. Chen and Y. Yu, *ACS Sustain. Chem. Eng.*, 2017, **5**, 2516–2528.
44 J. Klankermayer, S. Wesselbaum, K. Beydoun and W. Leitner, *Angew. Chem., Int. Ed.*, 2016, **55**, 7296–7343.
45 C. Federsel, A. Boddien, R. Jackstell, R. Jennerjahn, P. J. Dyson, R. Scopelliti, G. Laurenczy and M. Beller, *Angew. Chem., Int. Ed.*, 2010, **49**, 9777–9780.
46 C. Ziebart, C. Federsel, P. Anbarasan, R. Jackstell, W. Baumann, A. Spannenberg and M. Beller, *J. Am. Chem. Soc.*, 2012, **134**, 20701–20704.
47 P. Daw, S. Chakraborty, G. Leitus, Y. Diskin-Posner, Y. Ben-David and D. Milstein, *ACS Catal.*, 2017, **7**, 2500–2504.
48 Z. Liu, Z. Yang, Z. Ke, X. Yu, H. Zhang, B. Yu, Y. Zhao and Z. Liu, *New J. Chem.*, 2018, **42**, 13933–13937.
49 Z. He, H. Liu, H. Liu, Q. Qian, Q. Meng, Q. Mei and B. Han, *ChemCatChem*, 2017, **9**, 1947–1952.
50 H. Liu, Q. Mei, Q. Xu, J. Song, H. Liu and B. Han, *Green Chem.*, 2017, **19**, 196–201.
51 M. A. Affan and P. G. Jessop, *Inorg. Chem.*, 2017, **56**, 7301–7305.
52 L. Zhang, Z. Han, X. Zhao, Z. Wang and K. Ding, *Angew. Chem., Int. Ed.*, 2015, **54**, 6186–6189.
53 K. Zhang, L. Zong and X. Jia, *Adv. Synth. Catal.*, 2021, **363**, 1335–1340.
54 A. A. Dabbawala, N. Sudheesh and H. C. Bajaj, *Indian J. Chem., Sect. A:Inorg., Bio-inorg., Phys., Theor. Anal. Chem.*, 2015, **54A**, 753–756.
55 K. Kudo, H. Phala, N. Sugita and Y. Takezaki, *Chem. Lett.*, 1977, **6**, 1495–1496.
56 Y. Zhang, J. Wang, H. Zhu and T. Tu, *Chem.–Asian J.*, 2018, **13**, 3018–3021.
57 S. Schreiner, J. Y. Yu and L. Vaska, *J. Chem. Soc., Chem. Commun.*, 1988, 602–603.
58 S. Schreiner, J. Y. Yu and L. Vaska, *Inorg. Chim. Acta*, 1988, **147**, 139–141.
59 M. Minato, D. Y. Zhou, K. I. Sumiura, R. Hirabayashi, Y. Yamaguchi and T. Ito, *Chem. Commun.*, 2001, **1**, 2654–2655.
60 Y. Qin, H. Guo, X. Sheng, X. Wang and F. Wang, *Green Chem.*, 2015, **17**, 2853–2858.
61 M. A. Courtemanche, A. P. Pulis, É. Rochette, M. A. Légaré, D. W. Stephan and F. G. Fontaine, *Chem. Commun.*, 2015, **51**, 9797–9800.
62 M. Hulla and P. J. Dyson, *Angew. Chem., Int. Ed.*, 2020, **59**, 1002–1017.
63 A. Paparakis, R. C. Turnell-Ritson, J. S. Sapsford, A. E. Ashley and M. Hulla, *Catal. Sci. Technol.*, 2023, **13**, 637–644.
64 U. Jayarathne, N. Hazari and W. H. Bernskoetter, *ACS Catal.*, 2018, **8**, 1338–1345.
65 L. L. Zeonjuk, N. Vankova, A. Mavrandonakis, T. Heine, G. Röschenthaler and J. Eicher, *Chem.–Eur. J.*, 2013, **19**, 17413–17424.
66 L. Liu, B. Lukose, P. Jaque and B. Ensing, *Green Energy Environ.*, 2019, **4**, 20–28.
67 D. W. Stephan and G. Erker, *Angew. Chem., Int. Ed.*, 2010, **49**, 46–76.

68 F. Ebner, H. Wadepohl and L. Greb, *J. Am. Chem. Soc.*, 2019, **141**, 18009–18012.
69 K. Sordakis, C. Tang, L. K. Vogt, H. Junge, P. J. Dyson, M. Beller and G. Laurenczy, *Chem. Rev.*, 2018, **118**, 372–433.
70 S. Ishida, T. Hatakeyama, T. Nomura, M. Matsumoto, K. Yoshimura, S. Kyushin and T. Iwamoto, *Chem.–Eur. J.*, 2020, **26**, 15811–15815.
71 M. Hulla, G. Laurenczy and P. J. Dyson, *ACS Catal.*, 2018, **8**, 10619–10630.
72 G. Gastelu, D. Savary, M. Hulla, D. Ortiz, J. G. Uranga and P. J. Dyson, *ACS Catal.*, 2023, **13**, 2403–2409.
73 A. E. Finholt and E. C. Jacobson, *J. Am. Chem. Soc.*, 1952, **74**, 3943–3944.